Redox Processes in Early Earth Accretion and in Terrestrial Bodies

Kevin Righter[1], Christopher D. K. Herd[2] and Asmaa Boujibar[3]

1811-5209/20/0016-0161$2.50 DOI: 10.2138/gselements.16.3.161

The Earth is a unique rocky planet with liquid water at the surface and an oxygen-rich atmosphere, consequences of its particular accretion history. The earliest accreting bodies were small and could be either differentiated and undifferentiated; later larger bodies had formed cores and mantles with distinct properties. In addition, there may have been an overall trend of early reduced and later oxidized material accreting to form the Earth. This paper provides an overview—based on natural materials in our Earthbound sample collections, experimental studies on those samples, and calculations and numerical simulations of differentiation processes—of planetary accretion, core–mantle equilibration, mantle redox processes, and redox variations in Earth, Mars, and other terrestrial bodies.

KEYWORDS: accretion, oxygen fugacity, differentiation, core formation

The current make-up of the inner solar system ranges from airless and dry Mercury to oxygen-rich atmosphere and watery Earth. The ultimate critical controlling factor on this configuration is the early history of inner solar system bodies. Redox processes control the distribution and solubility of the key elements within both metallic and silicate liquids, such elements having the potential to react at depth or be outgassed later at the surface. An understanding of these equilibria and how they change with temperature and pressure affords insight into redox variations in the planets.

Iron provides important information about redox variation. The simple equilibrium Fe + O = FeO constrains the oxygen fugacity (f_{O_2}) within the inner solar system, commonly portrayed on a Prior diagram (e.g., Prior 1916). A Prior diagram can show the variation in the proportions of reduced (Fe metal) and oxidized (FeO and Fe_2O_3) iron that is present in meteorites (FIG. 1A). The range of f_{O_2} documented in planetary materials varies from iron–wustite (IW) from minus 8 to plus 7 (Righter et al. 2016): the IW+7, for example, refers to the oxygen fugacity (f_{O_2}) being 7 log units above that defined by the iron–wüstite (Fe–FeO) buffer. This convenient shorthand notation will be used throughout this paper. The variation of the distribution of Fe and FeO is also seen in terrestrial planets through correlations between FeO content of the mantle and the mass fraction of Fe-rich cores in Vesta (18%), Mars (21%), Earth and Venus (~30%) and Mercury (70%) (FIG. 1B). The causes of the different Fe/FeO distributions include variation in building block materials; redox equilibria that involve H, C, S, O, and Si; and planetary dynamics. Here, we will discuss these three topics and show how they can explain the variations we see in our solar system.

PLANETARY BUILDING BLOCKS

Terrestrial planet formation is thought to occur in three main stages: accretion of gas and dust, formation of planetesimals, merging of larger bodies in a late impact stage (FIG. 2). Because we have samples of materials from each of these stages, we can place f_{O_2} constraints on the building blocks that may have been present during planetary growth by examining mineral, melt, or trace element equilibria that are redox sensitive (Righter et al. 2016).

The first stage is represented by components in chondrites (i.e., the calcium aluminum–rich inclusions, or CAIs; the chondrules themselves; and the matrix) and primitive dust particles. Calcium aluminum–rich inclusions are considered to be the first crystalline materials to have condensed in equilibrium with the gaseous solar nebula at low pressures. They are made of refractory minerals such as spinel, clinopyroxene, melilite, perovskite, and anorthite. All of these first-stage materials exhibit a remarkable range of f_{O_2} from IW–8 (CAI fassaitic pyroxene) and upwards to metal-rich carbonaceous chondrite (CH) metal (IW–5.5), enstatite-rich chondrite (EL3) olivine (IW–6.5 to IW–4.5), the "Inte" Stardust particle (IW–6), inclusions in carbonaceous chondrites (IW–5 to IW–1.5), chondrules in ordinary and carbonaceous chondrites (IW–4 to 0), to Rumuruti-type chondrites (e.g., Righter et al 2016), GEMS (glass with embedded metal and sulfides) and oxidized Stardust particles (IW–3 to IW+1.5). This wide range of values spans ten logf_{O_2} units including solar values near IW–7 (Righter et al. 2016 and references therein) (FIG. 2 TOP).

The second stage is represented by samples of planetesimals such as meteorites from differentiated and undifferentiated bodies. As with the first stage, such materials span a wide f_{O_2} range from aubrites (IW–7 to –5), various iron meteorite groups (IW–4 to –2), acapulcoite/lodranite and winonites

1 NASA Johnson Space Center
2101 NASA Parkway
Houston, TX, 77058, USA
E-mail: kevin.righter-1@nasa.gov

2 University of Alberta
Department of Earth and Atmospheric Sciences
1-26 Earth Sciences Building
Edmonton, AB, T6G 2E9, Canada
E-mail: herd@ualberta.ca

3 Earth and Planets Laboratory
Carnegie Institution for Science
5251 Broad Branch Road NW
Washington DC 20015-1305, USA
E-mail: aboujibar@carnegiescience.edu

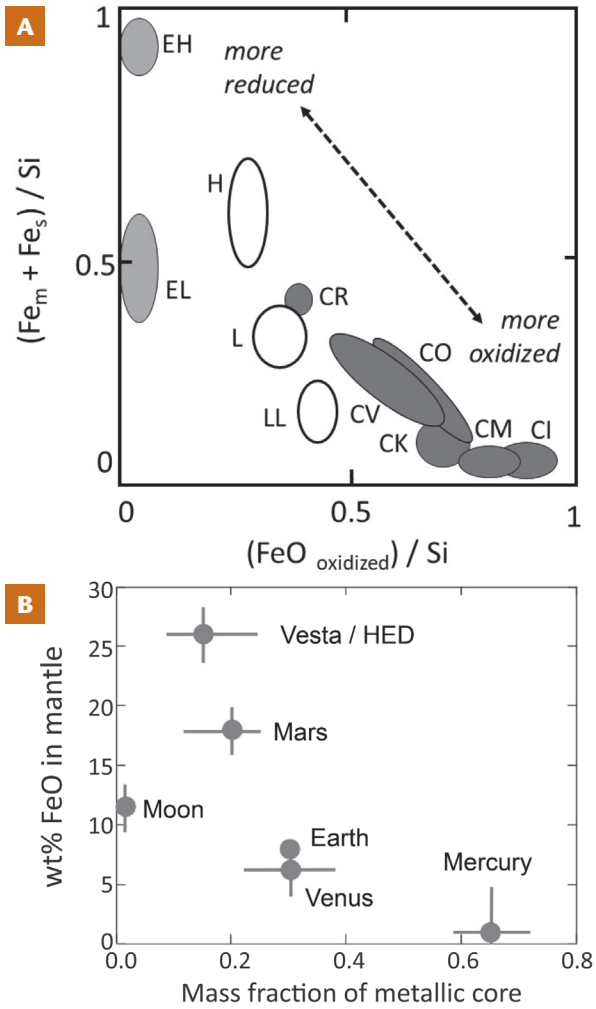

Figure 1 (**A**) A Prior (or Urey–Craig) diagram illustrating the negative correlation between reduced Fe (in metal, Fe_m; and sulfide, Fe_s) and oxidized Fe (as FeO), both normalized to Si. Abbreviations: EH and EL are enstatite chondrites (light grey ellipses); H, L, and LL are ordinary chondrites (white ellipses); CR, CV, CO, CK, CM, and CI are varieties of carbonaceous chondrites (dark grey ellipses). (**B**) Mass fraction of metallic core and mantle FeO are roughly correlated for the terrestrial planets and an asteroid (Vesta). Abbreviation: HED = howardite–eucrite–diogenite meteorite group, as derived from asteroid 4 Vesta. A notable exception is Earth's Moon, which has a very small core, presumably due to its unique origin by impact process. Modified from Righter et al. (2006).

(IW–3 to –1), ureilites (IW–3 to IW), the howardite–eucrite–diogenite clan and pallasites (IW–2 to –0.5), brachinites and related Graves Nunataks 06128/9 achondrites (IW–1 to IW+0.5), angrites (IW+1), to the thermally metamorphosed CK chondrites (IW+2 and higher; not shown in Fig. 2). Samples from Ceres may exhibit similar oxidation states to those of type 2 carbonaceous chondrites, given their similar mineralogy (McSween et al. 2018), and would, thus, fall as low as IW–3 for fayalite formation to as high as IW+3 for formation of smectite, saponite, phyllosilicates and magnetite. Samples from this stage also span an f_{O_2} range similar to that of the first stage materials of nearly 10 log units (Righter et al. 2016 and references therein) (Fig. 2 middle) and are also equilibrated at relatively low pressures.

The third stage is the formation of the planets themselves, in which case we have samples from Earth, Moon, and Mars, and remote spacecraft data for Mercury and Venus. For Earth, a great body of data has defined a wide range of oxygen fugacities that start near IW for continental xenoliths and ocean floor peridotites, extending to higher values for subduction zone mantle and hot spots (Kilauea, Hawaii, USA), to the highest values in magmas derived from metasomatized (oxidized) mantle (IW+4 to IW+8). Samples from Mars include picritic and basaltic rocks (the shergottite meteorites), cumulate clinopyroxenites (nakhlites) and some older crustal lithologies (orthopyroxenite and breccia). These samples collectively span over six logf_{O_2} units from IW–2 to IW+5. Venus has a similar core mass and core-to-mantle proportion to that of Earth, and we have some constraints on Venusian mantle FeO content from analyses of surface basalts. These crude constraints suggest that Venus, without plate tectonics and, thus, without recycling of surface volatiles to oxidize the mantle, may have f_{O_2} near that of Earth's early interior, perhaps IW–2 to IW–1. Mercury on the other hand, has S enrichment and FeO depletion at the surface, and possesses a large metallic core. The combination of these observations, and the fact that high S and low FeO silicate melts are favored at very low f_{O_2}, suggests that Mercury may have experienced f_{O_2} from IW–6 to IW–3 (Righter et al. 2016 and references therein) (Fig. 2 bottom). Finally, Earth's moon exhibits a narrow f_{O_2} range between IW and IW–2, despite having a very small metallic core. However, its formation in a giant impact involving the proto-Earth is somewhat unique.

Some redox variations in planets are caused by processes in relatively shallow crustal rocks, and knowledge of these processes can help to understand how initial planetary redox values can be modified. Thus, variations in redox states can, ultimately, be used to reveal information about planetary interiors. For example, applying multiple oxybarometers to certain shergottites (coexisting oxides, Fe^{3+}/Fe^{2+} in melts, olivine–pyroxene–spinel equilibria) shows that their redox state likely increased by two to three logf_{O_2}units during degassing (e.g., Righter et al. 2016; Castle and Herd 2017). On the other hand, nakhlites may record evidence of a reduction sequence caused by degassing of S_2, which is known to cause reduction in lunar basalts, eucrites, and ordinary chondrites (Righter et al. 2016 and references therein). If gaseous species (e.g., S^0) have different valences to species dissolved in a silicate melt (e.g., S^{2-}), then degassing can lead to a change in redox of the degassed magma. Thus, the difference in these two sequences ultimately lies in the different magmatic volatiles (e.g., Cl, H_2O, S) that may have been dissolved and degassed. This must be kept in mind when interpreting planetary basalt samples, such as those from Mars (and the Moon, Vesta, etc.).

Once degassing effects are recognized and accounted for, the inferred redox conditions of initial crystallization of the shergottite magmas provide insights into the f_{O_2} of Martian mantle sources (Castle and Herd 2017) and yield interesting insights into the interplay between building block composition, planetary size, and redox equilibria when compared with Earth. Correlations between time-integrated incompatible element enrichment and redox conditions strongly suggest the formation of mantle sources with linked geochemical and redox variations during initial fractionation of the silicate portion of Mars, most likely via magma ocean crystallization, over the f_{O_2} range of ~IW–1 to IW+2 (e.g., Castle and Herd 2017). Such sources are then left undisturbed until magma genesis, ascent, and eruption of the shergottites during the latter half of Mars' history (<2,400 Ma). The preservation of

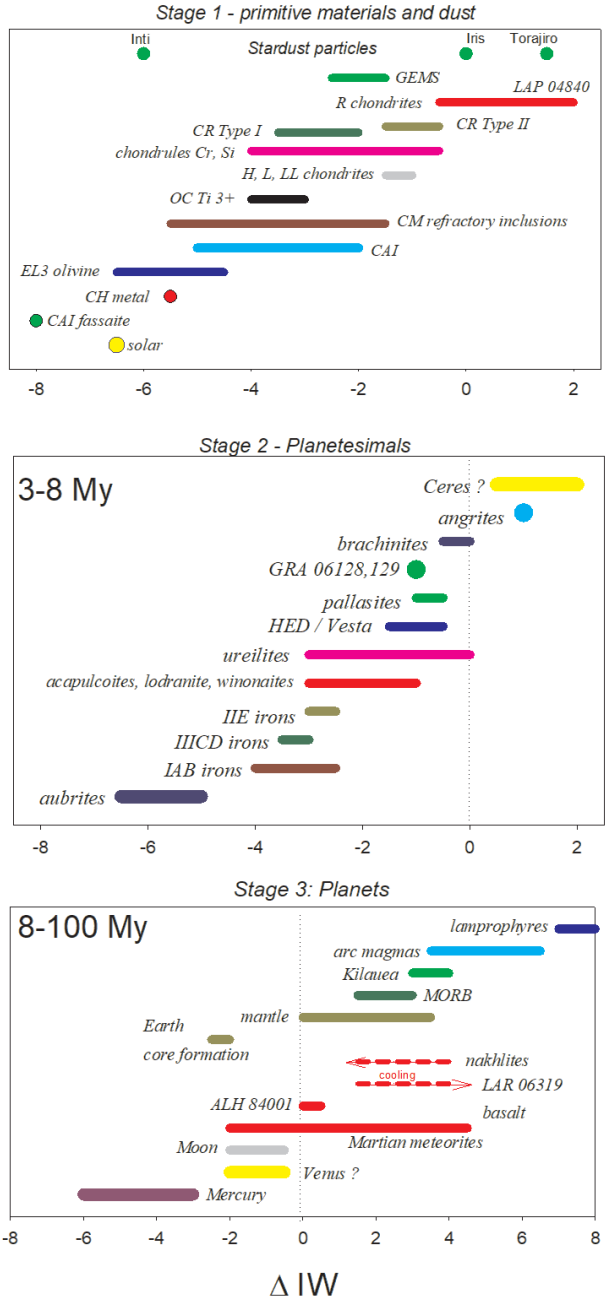

FIGURE 2 Range of oxygen fugacity recorded in planetary materials during the three main stages of accretion and planet building: (**UPPER**) Stage 1 is primitive materials and dust; (**MIDDLE**) Stage 2 is planetesimals; (**LOWER**) Stage 3 is planets. Abbreviations: HED, CH, CK, CM, CR, H, L, LL, and EL refer to the meteorite groups as in FIGURE 1; CAI = calcium aluminum–rich inclusions; OC = ordinary chondrite; Type I and Type II refer to the chondrules types in CR chondrites; GEMS = glass with embedded metal and sulfides; IIE, IIICD, and IAB refer to iron meteorite groups that contains silicate inclusions; MORB = mid ocean ridge basalt. Location abbreviations: GRA = Graves Nunataks; ALH =Allan Hills; LAP = LaPaz Icefield; LAR = Larkman Nunataks. These locations are for the dense collection areas in Antarctica where these meteorites (identified by number) were collected. Vertical sequence is f_{O_2} increasing upwards. ORIGINAL REFERENCES AND DETAILED DESCRIPTIONS OF SAMPLES AND MEASUREMENTS CAN BE FOUND IN RIGHTER ET AL. (2016).

such source characteristics over billion-year timescales is consistent with limited convection and mixing in the Martian mantle relative to Earth. More oxidized lithologies are generally produced through degassing, although early formed (~4,400 Ma) alkali basalt clasts in the Martian breccia have the highest recorded f_{O_2} for a Mars lithology, ~IW+5 (McCubbin et al. 2016). This might reflect conditions during formation of the primitive Martian crust.

In contrast, the much more vigorous convection and mixing within the Earth's mantle has apparently obliterated most early formed geochemical signatures (e.g., ^{142}Nd, ^{182}W) (Mundl et al. 2017). Furthermore, the dominant control on early mantle redox may have been the disproportionation of Fe^{2+} and the loss of metallic iron to the core, thereby oxidizing the lower mantle by several logf_{O_2} units immediately after core formation (e.g., Wood et al. 2006). Such a process would not occur within Mars due to its smaller size, because the disproportionation mechanism typically works only at pressures higher than those in the deep Martian mantle (Wood et al. 2006). For Earth, the progressive mixing of an oxidized lower mantle with a reduced upper mantle may be the cause of secular oxidation from ~IW+3 to IW+4.5 starting at ~3,500 Ma. Such a process may have played a role oxidizing the Earth's atmosphere at ~2,400 Ma (Nicklas et al. 2019). Thus, due to differences in planetary size, dynamics, and conditions of formation, primordial geochemical or redox mantle variations on Mars have been preserved whereas those in the Earth have been largely erased.

An interesting observation of materials from these three planetary formation stages is that they all record nearly the same range of f_{O_2} from IW–7 to IW+2, suggesting that the starting materials for planet growth may have had a direct influence on the end products. However, samples from Earth and Mars record the highest f_{O_2} values, which may mean that oxidation in the Earth may have been caused by later processes such as aqueous alteration, metasomatism, and recycling, whereas Mars may have had an oxidized early crust through degassing.

HIGH *P–T* REDOX EQUILIBRIA (METAL–SILICATE)

Planetary Fe-rich cores can contain significant amounts of light elements, including Si, S, O, C, and H. The presence of light elements is required to explain the density deficit of the Earth's core (Poirier et al. 1994). For Mars' core, the presence of S was proposed to explain geophysical data such as its moment of inertia (Sanloup et al. 1999). Experiments at high pressure and temperature that can replicate the chemical equilibria that occurs during core segregation confirm that light elements can be incorporated into core-forming Fe alloys in substantial concentrations (Poirier 1994). Reaction and equilibration of and between a silicate mantle and a metal core can be visualized through simple equilibria, such as:

$$Fe_{(metal)} + \tfrac{1}{2}O_2 = FeO_{(silicate)} \quad (1)$$

$$SiO_{2(silicate)} = Si_{(metal)} + O_2 \quad (2)$$

$$FeO_{(silicate)} = Fe_{(metal} + O_{(metal)} \quad (3)$$

$$FeO_{(silicate)} + \tfrac{1}{2}S_2 = FeS_{(metal)} + \tfrac{1}{2}O_2 \quad (4)$$

$$C_{(metal)} + O_2 = CO_{2(silicate)} \quad (5)$$

None of these equilibria alone are dominant: all are important when considering multicomponent equilibria that can be understood through appropriate experimental studies. These equilibria control the composition and size of the core and the composition and volatile content of

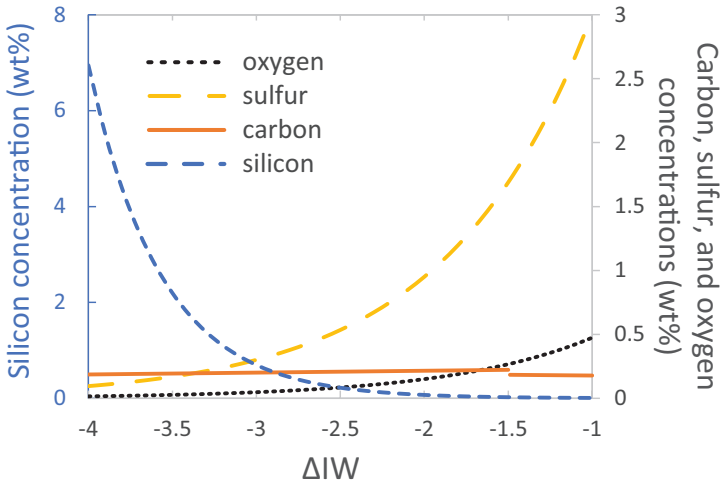

Figure 3 Role of oxygen fugacity (f_{O_2}) on the abundances of four light elements (C, S, O, Si) in an Fe alloy equilibrated with silicate at 5 GPa and 2,000 K on a graph of element concentrations versus change in the iron–wüstite buffer (ΔIW). The Si concentration (blue curve and left axis) decreases with the f_{O_2}; the concentrations of O and S (black and yellow curves, right axis) are correlated with the f_{O_2}. The abundance of C in Fe alloy is relatively weakly correlated with the oxygen fugacity. The degree of melt polymerization (as measured by the nonbridging oxygen per tetrahedrally coordinated cation parameter) and sulfide capacity (log C_S) were fixed at 2.56 and −5.324, respectively, as expected for the chemical composition of the Earth's mantle. Sulfur partitioning depends on the FeO concentration in the silicate melt (Boujibar et al. 2019), which was calculated at each f_{O_2} using Reactions (1) and (4) (see text). We used γ_{FeO}^{sil} = 1.7 and calculated γ_{Fe}^{met} using the online metal activity calculator (https://norris.org.au/expet/metalact/). Elements S, O, and Si were calculated using expressions presented by Boujibar et al. (2019), and C was calculated according to Li et al. (2016), all of which are based on data acquired on samples from a wide range of P–T–f_{O_2} conditions. The slight discontinuity in the C curve is due to the use of two expressions from Li et al. (2016): one for low f_{O_2} (<IW–1.5), and one for high f_{O_2} (>IW–1.5). To calculate S, C, and Si concentrations in metals from partition coefficients, we considered Earth's mantle values for S (200 ppm, from Palme and O'Neill 2014), C (765 ppm, from Marty et al. 2012), Si (45 wt%, from Palme and O'Neill 2014) and H_2O (300 ppm, from Cabral et al. 2014).

the mantle. Indeed, as a planet grows and a magma ocean deepens, the accreting material may contain H_2O or CO_2 that can oxidize the core-forming metal to FeO:

$$Fe + H_2O = FeO + H_2 \quad (6)$$

$$2Fe + CO_2 = 2FeO + C \quad (7)$$

In this way, core size and composition can change considerably compared to the original building blocks (Righter et al. 2006). This approach has been used to model the building blocks of Mars, whilst also matching core size, mean density, mean moment of inertia, and tidal response (Liebske and Khan 2019).

The S, C, Si, and O content of a planetary core can change dramatically with changes in f_{O_2}. These elements exhibit a trade-off in their solubility in Fe metal at the high pressures and temperatures relevant to planetary accretion. We illustrate this point with calculations of the core concentrations of S, C, Si, and O for the P–T conditions and composition of a planetesimal, but at variable f_{O_2}. Over the last few decades, the scientific community has constructed a significant body of high-P–T experimental data on metal–silicate equilibria. These data can be used to predict light element incorporation into Fe alloys across a wide range of pressure, temperature, oxygen fugacity, and chemical composition.

Partitioning of Si, O, S, and C between metal and silicate is described by the reactions shown in Equations (2), (3), (4), and (5), where the partition coefficient (via the equilibrium constant of each reaction) can be related to T, P, and oxygen fugacity (f_{O_2}); the activities of these elements in the metal and silicate can be calculated using semi-empirical expressions derived by Boujibar et al. (2019) and Li et al. (2016). To illustrate the effect of variable f_{O_2} on the corresponding core composition (in terms of Si, O, S and C), concentrations in liquid metal equilibrated with peridotitic silicate melt at f_{O_2} from IW–4 to IW–1 and constant P–T conditions (5 GPa, 2,000 K) were calculated using expressions from these two studies (Fig. 3). The resulting calculations show that oxygen fugacity has a strong effect on the solution of Si, O, S, and C in Fe metal alloys (Fig. 3). Carbon partitioning is less sensitive to f_{O_2} and its abundance in the metal remains relatively constant within each f_{O_2} range below and above IW–1.5. Conversely, whereas Si concentration in the metal is negatively correlated with f_{O_2}, S and O abundances increase with the f_{O_2}. At a low f_{O_2}, such as IW–4, metals contain 7 wt% Si, and less than 0.2 wt% S, C, or O. For oxidized conditions, such as IW–1, Si in metal is very low (< 0.007 wt%), whereas the concentrations of S and O can reach 3 wt% and 0.5 wt%, respectively. It is important to note that the abundance of each light element is calculated assuming that no other light element is in the Fe alloy, in order to isolate the effect of f_{O_2} and investigate evolutionary trends independently from chemical composition. However, because the partitioning of all four considered elements depends on the abundance of at least one other light element (Boujibar et al. 2019), the cumulative effect of f_{O_2} is more complex and requires iterative calculations. Moreover, core segregation is a continuous process

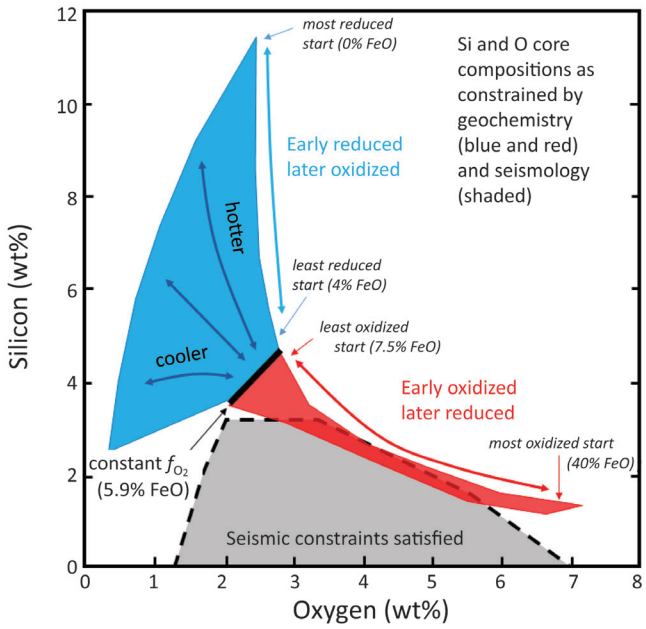

Figure 4 Light-element (Si and O) compositions for Earth's core that satisfies both geochemistry (colored bands) and seismology (black dashed line and gray background). The geochemically consistent cores are generated from multistage core-formation models, for various thermal conditions, and for increasing or decreasing magma ocean FeO contents (see Badro et al. 2015). The seismologically consistent composition space consists of the area delimited by the black dashed line. Models that start with more reduced low FeO magma oceans and that become more oxidizing during accretion result in relatively Si-rich cores, whereas models that start with more oxidized high-FeO magma oceans and that become more reduced during accretion (low FeO magma ocean) result in a relatively O-rich core. Redrawn after Badro et al. (2015).

where pressure and temperature increase over the course of accretion. These parameters are important to consider when addressing the chemistry of planetary cores.

An example of core formation at more extreme conditions is represented by the Earth. Because Si and O dissolve into Fe alloy at higher *P*–*T* conditions, and Si at more reduced conditions, these two elements have been used to show that Earth's density deficit (or solubility of a light element in the core) might be satisfied by some combination of Si and O, which covers a wide range of conditions (Fig. 4). This could also be true for S and C, but their availability is limited by cosmochemical constraints. Thus, Si and O—both major elements—provide the main constraints on Earth's core composition.

Another aspect of core-forming equilibria involving light elements, such as H and C, is the speciation of the associated volatile phase. For example, H_2O is very low in reduced systems even near the IW buffer, whereas H_2O is predominant in the H–O system at more oxidized conditions near the hematite–magnetite (HM) buffer (e.g., Behrens and Gaillard 2006). Similarly, CO_2 solubility in peridotite melt is strongly dependent on f_{O_2} and is <1 ppm at IW–2 but rises to >1,000 ppm at IW+1 (Dasgupta et al. 2013). These speciation effects and dependence upon f_{O_2} show that the dissolved and potentially degassed volatiles, and, thus, the composition of planetary atmospheres, are also strongly dependent on f_{O_2}.

PLANETARY ACCRETION MODELS

The first quantitative accretion models for Earth involved two components (Wänke 1981): an early reduced (metal-rich) component A, and a late oxidized (oxide-bearing) component B. The two-component mixture satisfied the overall chemical traits of the Earth. Such scenarios received some support from planetary dynamics where "feeding zones" extended outwards from Earth's local portion of the solar system to include more material from a larger heliocentric distance (Wetherill 1990). This shift from reduced state to oxidized state as *P* and *T* increased during accretion is also seen in the work of Fischer et al. (2017), who tested models of accretion with various starting compositions and degrees of mixing. Fischer et al. (2017) demonstrated that if starting materials are more reduced then there is more Si in the final core, whereas if they are more oxidized, the Si content is lowered (and O content raised) (Fig. 5). Additionally, accretion models for the solar system such as the Grand Tack (where giant planet dynamics control the sources of materials available for inner solar system planet growth) see a larger input of oxidized material from the outer solar system as accretion proceeds (Walsh et al. 2012). However, heterogeneous accretion models are not the only variety to produce gradual oxidation with increasing distance from the Sun. The nebular condensation calculations of Saxena and Hrubiak (2014) also predict that a Mercury-like metal-rich body forms closest to the Sun, followed by intermediate Earth- and Venus-like planets with ~30% cores, and finally Mars-like bodies with more FeS and FeO that form further out from the Sun. It is clear that both planetary dynamics simulations and nebular condensation calculations produce redox gradients that resemble our inner solar system.

Given these constraints, we can look more generally at ideas for the accretion of planets. Due to the large core and the FeO-poor and S-rich surface materials characterized first by remote spectroscopy (e.g., Sprague et al. 1995) and then by *MESSENGER* (Izenberg et al. 2014), it is clear that Mercury is a reduced body that might have accreted from enstatite chondrite–like material, or some metal-rich building blocks

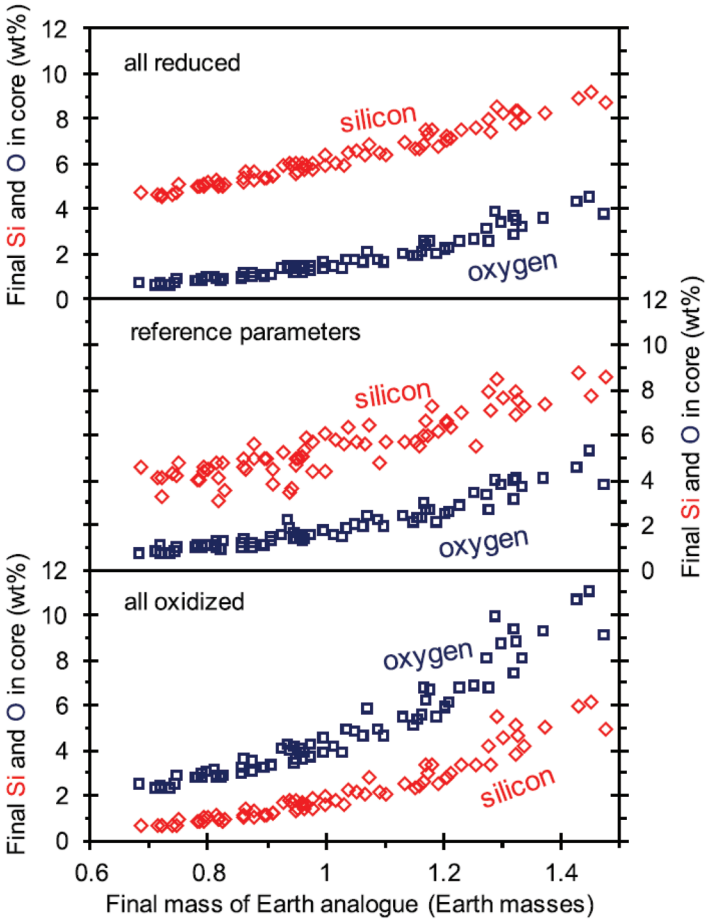

Figure 5 Final Si and O composition of the core as a function of Earth analogue mass for different oxidation states of the accreted material. Initial oxidation state of accreted material is the only core-formation model parameter varied between cases (panels); all other parameters were held fixed at their reference values. (**Upper panel**) All reduced starting materials; IW–3.5. (**Middle panel**) Reference set of model parameters (step function in oxidation state of starting materials). (**Lower panel**) All oxidized starting materials (IW–1.5). Navy blue squares: oxygen. Red diamonds: sillicon. The size of a planet largely controls its core Si and O contents, but accretion history also exerts an influence. Figure reprinted from Fischer et al. (2017), with permission from Earth and Planetary Science Letters.

such as the CH or CB chondrites (e.g., Brown et al. 2009). The metal enrichment may have also been caused, to some extent, by impact erosion of the Mercurian crust, leaving a metal-enriched body (Brown et al. 2009).

Earth must be made of material that will allow the 32% core but still leave a moderate amount of FeO in the mantle. Although two-component or heterogeneous accretion models can explain Earth's chemistry by variable f_{O_2} during accretion (e.g., Wänke 1981; Badro et al. 2015) (Fig. 5), several models have proposed that Earth is enstatite chondrite–like with FeO forming by oxidation of Fe metal as growth occurred (Javoy et al. 2010; Liebske and Khan 2019). That there are several processes and starting materials that can make Earth seems safe to say. Earth's formation is still an open topic without a clear paradigm. By analogy we can extend this argument to Venus, because we have so little detailed information about the Venusian interior.

Finally, Mars contrasts with Earth in that even 35 years ago geochemists realized it was easier to explain Mars' more oxidized and volatile-rich composition compared to Earth (Dreibus and Wänke 1985). Lodders and Fegley (1997) argued for 85% H chondrite along with 11% CV and 4% CI chondrite material. Sanloup et al. (1999) also argued for dominantly H chondrite but with the balance made up of EH chondrites. The most recent look at Mars' bulk composition, which also draws on extensive isotopic data that is now available for chondritic and other building blocks, shows that Mars could be accreted from a mixture of chondrites and an oxidized differentiated body. The chondritic material could have come from as many as 12 different meteorite groups contributing to the overall bulk composition (Liebske and Khan 2019).

The contrast between Earth, which could have formed mostly from material like enstatite chondrites, and Mars, which apparently formed from a mixture of diverse materials (including an important role for oxidized differentiated material), indicates that the redox properties of the planets really were controlled by all three processes highlighted above: their building blocks, high *P*–*T* redox equilibria, and the degree of mixing and accretion dynamics that affected the relevant portion of the inner solar system.

SUMMARY

Great strides have been made in understanding the role of redox equilibria and redox variation during planetary accretion. Although experimental studies have provided fundamental constraints on accretion and differentiation in planetary interiors, much work remains to be done to understand the phase equilibria of planetary cores and mantles at high pressures and temperatures, especially those containing volatiles such as H, C, S, and N. Additional understanding will come from new sample materials, such as meteorites and sample return missions, especially from Venus for which we currently have no samples and for which our knowledge of its exterior and interior is poor. Models and numerical calculations of the accretion process and a refined knowledge of the sources of materials that become accreted onto a planet will undoubtedly lead to new insights into redox variation within the inner solar system.

REFERENCES

Badro J, Brodholt JP, Piet H, Siebert J, Ryerson FJ (2015) Core formation and core composition from coupled geochemical and geophysical constraints. Proceedings of the National Academy of Sciences of the United States of America 112: 12310-12314

Behrens H, Gaillard F (2006) Geochemical aspects of melts: volatiles and redox behavior. Elements 2: 275-280

Boujibar A and 7 coauthors (2019) U, Th, and K partitioning between metal, silicate, and sulfide and implications for Mercury's structure, volatile content, and radioactive heat production. American Mineralogist 104: 1221-1237

Brown SM, Elkins-Tanton LT (2009) Compositions of Mercury's earliest crust from magma ocean models. Earth and Planetary Science Letters 286: 446-455

Cabral RA and 9 coauthors (2014) Volatile cycling of H_2O, CO_2, F, and Cl in the HIMU mantle: a new window provided by melt inclusions from oceanic hot spot lavas at Mangaia, Cook Islands. Geochemistry, Geophysics, Geosystems 15: 4445-4467

Castle N, Herd CD (2017) Experimental petrology of the Tissint meteorite: redox estimates, crystallization curves, and evaluation of petrogenetic models. Meteoritics & Planetary Science 52: 125-146

Dasgupta R (2013) Ingassing, storage, and outgassing of terrestrial carbon through geologic time. Reviews in Mineralogy and Geochemistry 75: 183-229

Dreibus G, Wänke H (1985) Mars, a volatile-rich planet. Meteoritics 20: 367-381

Fischer RA, Campbell AJ, Ciesla FJ (2017) Sensitivities of Earth's core and mantle compositions to accretion and differentiation processes. Earth and Planetary Science Letters 458: 252-262

Izenberg NR and 16 coauthors (2014) The low-iron, reduced surface of Mercury as seen in spectral reflectance by MESSENGER. Icarus 228: 364-374

Javoy M and 10 coauthors (2010) The chemical composition of the Earth: enstatite chondrite models. Earth and Planetary Science Letters 293: 259-268

Li Y, Dasgupta R, Tsuno K, Monteleone B, Shimizu N (2016) Carbon and sulfur budget of the silicate Earth explained by accretion of differentiated planetary embryos. Nature Geoscience 9: 781-785

Liebske C, Khan A (2019) On the principal building blocks of Mars and Earth. Icarus 322: 121-134

Lodders K, Fegley B Jr (1997) An oxygen isotope model for the composition of Mars. Icarus 126: 373-394

Marty B (2012) The origins and concentrations of water, carbon, nitrogen and noble gases on Earth. Earth and Planetary Science Letters 313-314: 56-66

McSween HY Jr. and 9 coauthors (2018) Carbonaceous chondrites as analogs for the composition and alteration of Ceres. Meteoritics & Planetary Science 53: 1793-1804

Mundl A and 7 coauthors (2017) Tungsten-182 heterogeneity in modern ocean island basalts. Science 356: 66-69

Nicklas RW and 8 coauthors (2019) Secular mantle oxidation across the Archean-Proterozoic boundary: evidence from V partitioning in komatiites and picrites. Geochimica et Cosmochimica Acta 250: 49-75

Palme H, O'Neill H (2014) Cosmochemical estimates of mantle composition. In: Carlson RW (ed) The Mantle and Core. Treatise on Geochemistry, Volume 3, 2nd edition, Elsevier Press, pp 1-39

Poirier J-P (1994) Light elements in the Earth's outer core: a critical review. Physics of the Earth and Planetary Interiors 85: 319-337

Prior GT (1916) On the genetic relationship and classification of meteorites. Mineralogical Magazine and Journal of the Mineralogical Society 18: 26-44

Righter K, Drake MJ, Scott ERD (2006) Compositional relationships between meteorites and terrestrial planets. In: Lauretta DS, McSween HY Jr (eds) Meteorites and the Early Solar System II. University of Arizona Press, pp 803-828

Righter K, Sutton SR, Danielson L, Pando K, Newville M (2016) Redox variations in the inner solar system with new constraints from vanadium XANES in spinels. American Mineralogist 101: 1928-1942

Sanloup C, Jambon A, Gillet P (1999) A simple chondritic model of Mars. Physics of the Earth and Planetary Interiors 112: 43-54

Saxena SK, Hrubiak R (2014) Mapping the nebular condensates and the chemical composition of the terrestrial planets. Earth and Planetary Science Letters 393: 113-119

Sprague AL, Hunten DM, Lodders K (1995) Sulfur at Mercury, elemental at the poles and sulfides in the regolith. Icarus 118: 211-215

Walsh KJ, Morbidelli A, Raymond SN, O'Brien DP, Mandell AM (2012) Populating the asteroid belt from two parent source regions due to the migration of giant planets—"The Grand Tack". Meteoritics & Planetary Science 47: 1941-1947

Wänke H (1981) Constitution of terrestrial planets. Philosophical Transactions of the Royal Society of London, Series A: Mathematical, Physical and Engineering Sciences 303: 287-302

Wetherill GW (1990) Formation of the Earth. Annual Review of Earth and Planetary Sciences 18: 205-256

Wood BJ, Walter MJ, Wade J (2006) Accretion of the Earth and segregation of its core. Nature 441: 825-833